

# Transverse momentum dependent factorization for lattice observables

Alexey A. Vladimirov and Andreas Schäfer  
*Institut für Theoretische Physik, Universität Regensburg,  
D-93040 Regensburg, Germany*

Using the soft collinear effective field theory approach, we derive the factorization theorem for the quasi-transverse momentum dependent (quasi-TMD) operator. We check the factorization theorem at one-loop and derive corresponding coefficient function and anomalous dimensions. The factorized expression is build of the physical TMD distribution, and a non-perturbative lattice related factor. We demonstrate that lattice-related functions cancel in appropriately constructed ratios. These ratios could be used to explore various properties of TMD distributions, the main of which is the non-perturbative evolution kernel. A discussion of such ratios and the related continuum properties of TMDs is presented.

## I. INTRODUCTION

Over the last years continuous progress in theory and phenomenology of a transverse momentum dependent (TMD) factorization theorem made it a valuable tool for analysis and prediction of many observables (for a review see [1]). It has been demonstrated that the TMD factorization approach accurately describes the data in a broad range of energies and a wide spectrum of processes [2–6]. Conceptually, the TMD factorization [7, 8] is different from the collinear factorization and gives rise to a number of specific novel effects. In this article, we apply TMD factorization for a certain class of operators suitable for evaluation by QCD lattice methods.

A nucleon has eight leading twist TMD distributions, each of which depends on a transverse variable and momentum fraction  $x$ , to that end, the purely experimental determination of all of TMD distributions is a highly non-trivial task. Therein, the prospects for obtaining complementary information from QCD lattice simulations look extremely promising, in particular, due to the possibility of measuring correlators directly in the coordinate space. In fact, the TMD factorization theorem we discuss and TMD distributions are naturally formulated in the coordinate space, despite the fact that their interpretation is usually given in the momentum space. From experimental data one can extract coordinate space information only via a Fourier transformation, resulting in a significant systematic error and model-bias. A good example for the encountered problems is the TMD evolution kernel  $\mathcal{D}(b)$  (also known as Collins-Soper(CS) kernel [9]). To extract the CS kernel from data one has to combine data from many experiments performed at varying energies. The current global pool of data gives access to energies from 1 to 150GeV [5]. However, the precision of the most part of the data is quite limited and their interpretation depends non-trivially on  $\mathcal{D}$ . The later is known up to  $\alpha_s^3$ -order in perturbation theory [10], but is poorly constraint beyond perturbative values of  $b$ . Even the shape of  $\mathcal{D}(b)$  is questionable (compare f.i. extractions in [5] and [6]). This problem can be resolved, or at least, reduced by lattice simulations.

Suggestions for lattice studies of TMD observables

were made long ago [11, 12]. At that time, however, some crucial assumptions were rather conjectural. Recently, such efforts were promoted to a higher level [13–15] with the formulation of appropriate factorization theorems. In all cases, one considers an equal-time analog of a TMD operator, which turns into an ordinary TMD operator after the boost. In this paper, we present a different analysis of the same operator within the TMD factorization approach, based on the  $q_T$ -dependent soft-collinear effective field theory (SCET II). We demonstrate that the TMD hadron tensor is more closely related to the suggested lattice observables than the TMD distributions making the use of TMD factorization approach advantageous. Using the TMD hadron tensor we present a construction which stresses the analogy between lattice observables and physical quantities used in the description of ordinary processes like the Drell-Yan process, utilizing the same terminology. Although the route of derivation of the factorized expression differs from [14, 15] we arrive at an equivalent result. Checking the factorized expression at one-loop level, we found that the perturbative parts are in complete agreement with [14].

Convergence of the derived factorized expression is bad due terms divergent at small- $x$ . Such a problem is quite common for factorization theorems for lattice observables. For example, the quasi-parton distribution functions (PDF) [16, 17] also suffer from this problem, as is discussed, e.g., in ref.[18]. In the TMD case, the small- $x$  divergent terms are more troublesome because they are enhanced by TMD evolution effect. This is unavoidable, since the hard scale in lattices problems is the parton momentum  $\sim xP$  leading to strong factorization breaking at small  $x$ .

The paper is split into three sections. In sec.II we define matrix elements suitable for lattice simulations and derive the factorized expression using SCET II. In sec.III we check factorization at one-loop level and derive the corresponding coefficient function at next-to-leading order (NLO). Finally, in sec.IV we discuss some properties of the ratios of matrix elements which have simpler properties and thus could serve to determine TMD distributions with less effort. We emphasize in particular the advantages of ratios at small-longitudinal separation.

## II. FACTORIZATION THEOREM

### A. Definition of the lattice observable.

The considered lattice observable reads

$$W_{f\leftarrow h}^{[\Gamma]}(b; \ell, L; v, P, S) = \frac{1}{2} \langle P, S | \bar{q}(b + \ell v) \Gamma \times [b + \ell v, b + Lv][b + Lv, Lv][Lv, 0] q(0) | P, S \rangle, \quad (1)$$

where  $|P, S\rangle$  is a single-hadron state with momentum  $P$  and spin  $S$ , and  $\Gamma$  is a Dirac matrix. The hadron species and the flavor of the quark field are specified by labels  $h$  and  $f$ .  $[x, y]$  is the straight gauge link between points  $x$  and  $y$ ,

$$[x, y] = P \exp \left( ig \int_0^1 dt (x - y)^\mu A_\mu(y + t(x - y)) \right). \quad (2)$$

The same object has been considered in [13–15, 19, 20]. Often, the matrix element (1) is called a quasi-TMD distribution in analogy to the quasi-parton distribution functions [16]. However, as we demonstrate in the next section, the structure of (1) does not remind a TMD distribution but rather a TMD hadronic tensor, such as the hadronic tensor for the Drell-Yan process or Semi-inclusive deep inelastic scattering (SIDIS). For that reason, we avoid the term quasi-TMD distribution, and denote (1) by the letter  $W$ .

The space-time orientation of different quantities in  $W$  is given in fig.1. The lattice operator must be an equal time operator and thus the vectors  $v^\mu$  and  $b^\mu$  do not have time-components. Consequently,  $b^2 < 0$  and  $v^2 < 0$ . The vectors  $P^\mu$  and  $v^\mu$  defines an analog of the scattering plane. The transverse vector  $b^\mu$  is orthogonal to them,

$$(v \cdot b) = 0, \quad (b \cdot P) = 0. \quad (3)$$

The vector  $b^\mu$  defined by (3) is restricted to a line, due to absence of time-components (except a special case when vectors  $v^\mu$ ,  $P^\mu$  and the time-direction lie in a plane). The situation is different for the physical kinematics where the scattering plane is formed by two time-like vectors and thus the vector  $b^\mu$  is restricted to a plane.

### B. Factorization limit.

The clear separation of collinear and soft field-modes within the hadron is a prerequisite for any TMD factorization theorem. It can be achieved by considering a fast moving hadron, for which anti-collinear components of field momenta are suppressed in comparison to collinear ones. To quantify this condition we write the momentum of a hadron as

$$P^\mu = P^+ \bar{n}^\mu + \frac{M^2}{2P^+} n^\mu, \quad (4)$$

where  $M$  is the mass of the hadron,  $n$  and  $\bar{n}$  are light-like vectors  $n^2 = \bar{n}^2 = 0$  (see also fig.1), normalized according

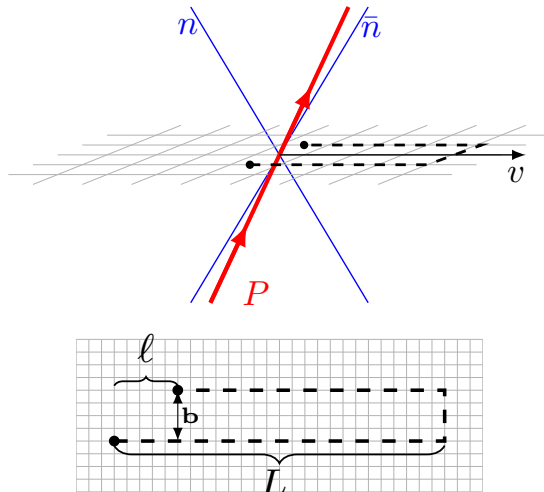


FIG. 1. Illustration for the definition of the matrix element  $W(b; \ell, L; v, P)$  (1). Dashed lines denotes the Wilson links, and black dots denotes the quark fields. Top and bottom illustrations correspond to side and top views relative to the gauge link plane.

to  $(n \cdot \bar{n}) = 1$ . Here, we use the standard notation of light-cone components of a vector  $a^\mu$ :

$$a^\mu = \bar{n}^\mu a^+ + n^\mu a^- + a_T^\mu. \quad (5)$$

So, the factorization limit requires

$$\frac{P^-}{P^+} = \frac{M^2}{2(P^+)^2} \sim \lambda^2 \ll 1. \quad (6)$$

with  $\lambda$  being the generic small parameter of SCET. In this regime the hadron momentum is almost light-like.

We also assume that the staple-shaped gauge links contour (1) is much longer than broad

$$b, \ell \ll L. \quad (7)$$

Under this assumption, the effects caused by the interaction with the transverse gauge link  $[b + Lv, Lv]$  are suppressed as  $b/L$  and  $\ell/L$ , and thus can be neglected. We then introduce a scalar field,  $H(x)$ , with the Lagrangian

$$\mathcal{L}_{HH} = H^\dagger (iv \cdot D) H + \mathcal{O}(L^{-1}), \quad (8)$$

and approximate the gauge-links  $[x, x + Lv]$  by the  $H$  propagator. In eq.(8),  $D_\mu$  is the QCD covariant derivative. The field  $H$  differs from a usual scalar heavy quark field [21] only by the fact that  $v^2 < 0$ .

In the notation (8), the similarity of the matrix element (1) with the ordinary hadron tensor for TMD factorization becomes transparent. We rewrite (1) as

$$W_{ij}(b; \ell, L; v, P) = \sum_X \langle P, S | J_i^\dagger(v\ell + b) | X \rangle \langle X | J_j(0) | P, S \rangle + \mathcal{O}(L^{-1}), \quad (9)$$

where  $W^{[\Gamma]} = \frac{1}{2} \text{Tr}(W\Gamma)$  and  $J_i$  is the heavy-to-light current

$$J_i(x) = H^\dagger(x) q_i(x). \quad (10)$$

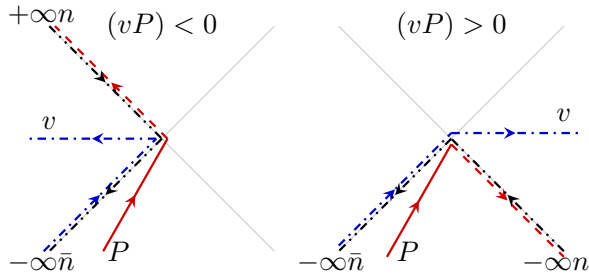


FIG. 2. Illustration for Wilson lines structure for operators  $J_i$  (13) and  $\bar{J}_i$  (15) in the plane  $(P, v)$ . Red (solid and dashed) color indicates the collinear fields, blue (dot-dashed) – anti-collinear fields and black (double-dot-dashed) – soft fields.

The structure of the first term in (9) resembles the structure of the hadron tensor for TMD cross-sections, with the main difference that there is only a single hadron. The second hadron is replaced by the “instant” field  $H$ .

### C. Field modes factorization and SCET current.

The analogy with the TMD hadron tensor (9) allows us to recapitulate the main points of the TMD factorization and apply it to the lattice case. To derive the factorized expression, we use the soft-collinear effective field theory with finite  $q_T$  (SCET II) approach, similarly to ref.[8].

In SCET II, one distinguishes collinear, anti-collinear and soft fields. At the leading term approximation, the fast-moving hadron is a composition of collinear fields ( $\xi$  for quarks and  $A_{c,\mu}$  for gluons). Their momentum components are of the structure

$$\partial_\mu \xi \sim \{1, \lambda^2, \lambda\} \xi, \quad \partial_\mu A_c \sim \{1, \lambda^2, \lambda\} A_c, \quad (11)$$

where the curly brackets contain light-cone components. The separation of transverse and collinear modes requires a clear hierarchy between corresponding momentum components. In the present case, the typical transverse momenta in diagrams are  $\sim b^{-1}$ . And, therefore, we have an additional constraint

$$\frac{1}{|b|P^+} \sim \lambda. \quad (12)$$

A priori it is not evident how to count the field  $H$  in terms of  $\lambda$  since a Wilson line does not carry a momentum. However, the situation becomes clear if one boosts the system such that  $P^- \rightarrow 0$ . Then the Wilson line  $H$  is turned towards the light-cone direction  $n$ . In the boosted frame, the  $v^+$ -component of  $v^\mu$  can be ignored and the field  $H$  can be approximately considered

as an anti-collinear Wilson line. Therefore, the fields  $H$  and collinear fields have no direct interaction but only through soft exchanges.

Using these counting rules we write the leading power SCET operator that corresponds to the current  $J_i$  (10)

$$J_i^{\text{SCET}}(x) = C_H(v \cdot \hat{p})(H^\dagger W_{\bar{n}}) Y_{\bar{n}}^\dagger Y_n (W_n^\dagger \xi_i)(x). \quad (13)$$

In this expression the collinear Wilson line

$$W_n(x) = P \exp \left( ig \int_{-\infty}^0 d\sigma n \cdot A_c(x + n\sigma) \right), \quad (14)$$

contains all gluons radiated by the collinear quark field. The anti-collinear Wilson line  $W_{\bar{n}}$  contains the gluons radiated by the  $H$ -field and is given by a similar expression with  $n \rightarrow \bar{n}$ . The Wilson lines  $Y$  are the result of the decoupling transformation [22]. They have analogous expression to (14) but build with soft gluon fields.

The coefficient  $C_H$  is the matching coefficient between SCET and QCD operators. It depends on the momentum of field  $\xi$  (in position space  $\hat{p}$  is an operator), and is independent on the quark flavor. At the leading order  $C_H = 1$ .

Expression (13) applies for  $(vP) > 0$ . If  $(vP) < 0$  the gluon fields are summed with the opposite sign (in comparison to (13)) and thus they form Wilson lines pointing to  $+\infty n$ . So, for the case  $(vP) < 0$  the SCET operator reads

$$\bar{J}_i^{\text{SCET}}(x) = \bar{C}_H(v \cdot \hat{p})(H^\dagger W_{\bar{n}}) Y_{\bar{n}}^\dagger \bar{Y}_n (\bar{W}_n^\dagger \xi_i)(x), \quad (15)$$

where

$$\bar{W}_n(x) = P \exp \left( ig \int_{+\infty}^0 d\sigma n \cdot A_c(x + n\sigma) \right), \quad (16)$$

and similarly for  $\bar{Y}$ . Alternatively, the directions of Wilson lines could be recovered by noting that in the  $P^- \rightarrow 0$  boosted frame, Wilson lines  $H$  point to the past (future) if  $(vP) > 0$  ( $(vP) < 0$ ). The visual representation of operator  $J$  and  $\bar{J}$  is shown in fig.2.

Combining (13) and (15) we write matching expression for the QCD current (10)

$$J_i(x) = \begin{cases} J_i^{\text{SCET}}(x) + \mathcal{O}(\lambda), & (vP) > 0, \\ \bar{J}_i^{\text{SCET}}(x) + \mathcal{O}(\lambda), & (vP) < 0. \end{cases} \quad (17)$$

Note, that different spinor components of  $\xi_i$  have different power counting. The large (small) components can be projected out by the matrix  $\gamma^- \gamma^+ / 2$  ( $\gamma^+ \gamma^- / 2$ ).

### D. Factorized expression.

Substituting the effective currents (17) into the expression (1) we obtain (here for  $(vP) > 0$ )

$$W_{f \leftarrow h}^{[\Gamma]}(b; \ell, L; v, P, S) = \left| C_H(\hat{p} \cdot v) \right|^2 \langle P, S | \left( \bar{\xi} W_n(b + \ell v) \frac{\Gamma}{2} W_n^\dagger \xi(0) \right) \left( H^\dagger W_{\bar{n}}(0) W_{\bar{n}}^\dagger H(b + \ell v) \right) \frac{\text{Tr}}{N_c} \left[ Y_n^\dagger Y_{\bar{n}}(b + \ell v) Y_{\bar{n}}^\dagger Y_n(0) \right] | P, S \rangle. \quad (18)$$

Here, we have performed a Fiertz transformation to recouple color indices, and have dropped color-covariant structures. The collinear, anti-collinear and soft fields operate on different Hilbert spaces, such that the total Hilbert space can be written as a direct product of three distinct Hilbert spaces [23, 24]. Doing so one has to correct for overlap in the field definitions in the soft region. The overlap contribution can be removed by the so-called zero-bin subtraction factor [25]. Additionally the fields can be Taylor-expanded in the slow (in comparison to other components) directions, which are determined by the counting rules (11). After these operations we obtain the following result

$$W_{f \leftarrow h}^{[\Gamma]}(b; \ell, L; v, P, S) = \left| C_H(\hat{p} \cdot v) \right|^2 \tilde{\Phi}_{f \leftarrow h}^{[\Gamma]}(b, lv^-; P, S) \tilde{\Psi}(b, lv^+; v) \frac{S(b)}{\text{Z.b.}} + \mathcal{O}(\lambda), \quad (19)$$

where

$$\Gamma' = \frac{1}{4} \gamma^+ \gamma^- \Gamma \gamma^- \gamma^+. \quad (20)$$

The functions are

$$\tilde{\Phi}_{f \leftarrow h}^{[\Gamma]}(b, x^-; P, S) = \langle P, S | \bar{q}(x^- n + b) [x^- n + b, -\infty n + b] \frac{\Gamma}{2} [-\infty n, 0] q(0) | P, S \rangle, \quad (21)$$

$$\tilde{\Psi}(b, x^+; v) = \langle 0 | H^\dagger(0) [0, -\infty \bar{n}] [-\infty \bar{n} + b, x^+ \bar{n} + b] H(x^+ \bar{n} + b) | 0 \rangle, \quad (22)$$

$$S(b) = \frac{\text{Tr}}{N_c} \langle 0 | [b, -n\infty + b] [-n\infty, 0] [0, -\bar{n}\infty] [-\bar{n}\infty + b, b] | 0 \rangle, \quad (23)$$

where we use the QCD fields since within its own Hilbert space each sector of SCET is equivalent to QCD. The zero-bin factor (denoted as Z.b.) removes the contribution from the overlap of soft and collinear modes. It is not known explicitly except for certain regularizations, f.i. in the  $\delta$ -regularization [8] where it is equivalent to the TMD soft factor.

The function  $\tilde{\Phi}$  is (a Fourier transform of) an unsubtracted TMD distribution. The function  $\tilde{\Psi}$  has an analogous structure. The only difference is that it measures a TMD distribution of a field  $H$ . For that reason we call it an (unsubtracted) instant-jet TMD distribution. The function  $S$  is the TMD soft factor. The expression (19) applies for  $(vP) > 0$  and thus,  $\tilde{\Phi}$  and  $S$  correspond to Drell-Yan kinematics. If  $(vP) < 0$  the Wilson line along  $n$  point to  $+\infty n$ , and  $\tilde{\Phi}$  and  $S$  correspond to SIDIS kinematics (and the coefficient function is replaced by  $\bar{C}_H$ ).

### E. Recombination of rapidity divergences.

Unsubtracted TMD distributions have rapidity divergences that appear due to the presence of infinite light-like Wilson lines separated in the transverse plane. Rapidity divergences are associated with the directions of Wilson lines. In the current case, there are two light-cone directions, and thus we introduce two regularization parameters  $\delta^+$  and  $\delta^-$ . These parameters regularize rapidity divergences associated with the directions  $n$  and  $\bar{n}$ , correspondingly. In the product of all functions in (19)

rapidity divergences cancel, and therefore, the last step of the factorization approach is to recombine rapidity divergences, and to introduce physical (aka finite) TMD distributions. In this procedure we follow ref.[26]. In what follows, we use  $\delta$ -regularization for rapidity divergences, but the same procedure can be performed for different kinds of regulators. The final result is independent of the regularization used.

In the expression (19) the rapidity divergences are present according to the following pattern (in this section we omit all arguments of function, except the ones related to rapidity divergences)

$$W = |C_H|^2 \tilde{\Phi}(\delta^+) \frac{S(\delta^+, \delta^-)}{\text{Z.b.}(\delta^+, \delta^-)} \tilde{\Psi}(\delta^-). \quad (24)$$

In ref.[26] it has been shown that rapidity divergences are structurally equivalent to ultraviolet divergences, and therefore, can be absorbed into a divergent factor  $R$ . Introducing rapidity renormalization factors into (24) we obtain

$$W = |C_H|^2 \tilde{\Phi}(\nu^+) S_0^{-1}(\nu^2) \tilde{\Psi}(\nu^-), \quad (25)$$

where  $\nu^\pm$  are the scales of rapidity-divergence renormalization, and

$$\tilde{\Phi}(\nu^+) = \tilde{\Phi}(\delta^+) R \left( \frac{\delta^+}{\nu^+} \right), \quad \tilde{\Psi}(\nu^-) = R \left( \frac{\delta^-}{\nu^-} \right) \tilde{\Psi}(\delta^-),$$

$$S_0^{-1}(\nu^2) = R^{-1} \left( \frac{\delta^+}{\nu^+} \right) \frac{S(\delta^+, \delta^-)}{\text{Z.b.}(\delta^+, \delta^-)} R^{-1} \left( \frac{\delta^-}{\nu^-} \right).$$

The function  $S_0$  depends on  $\nu^2 = 2\nu^+\nu^-$  due to Lorenz invariance. This expression is independent on  $\nu^\pm$  by definition, and each function here is finite. The dependence on  $\nu^\pm$  is given by renormalization group equation

$$\nu^+ \frac{d\tilde{\Phi}(\nu^+)}{d\nu^+} = \frac{\mathcal{D}}{2} \tilde{\Phi}(\nu^+), \quad (26)$$

where  $\mathcal{D}$  is the rapidity anomalous dimension [26], or CS-kernel [9]:

$$\mathcal{D} = \frac{1}{2} \frac{d \ln R}{d \ln \nu^+}. \quad (27)$$

The equation for  $\tilde{\Psi}$  is analogous.

Introducing the boost-invariant variables

$$\zeta = 2(p^+)^2 \frac{\nu^-}{\nu^+}, \quad \bar{\zeta} = 2\tilde{\mu}^2 (v^-)^2 \frac{\nu^+}{\nu^-}, \quad (28)$$

where  $p^+ \sim P^+$  (to be fixed later) and  $\tilde{\mu}$  is a scale with the dimension of mass. The parameter  $\zeta$  is the standard rapidity evolution parameter [7, 8, 26]. The parameter  $\bar{\zeta}$  is the analogous parameter for  $\Psi$ . Let us emphasize that the scale of rapidity divergences is associated with the collinear component of a momentum. However, as already discussed, no momentum is associated with the field  $H$ . The only momentum scale present in  $\Psi$  is the factorization scale. Therefore,  $\tilde{\mu} \sim \mu$ . In sec.III, we confirm the validity of this choice of parameters by a one-loop calculation. The dependence of the function  $\tilde{\Phi}(\zeta, \nu^2)$  on  $\zeta$  follows from (26) and reads

$$\zeta \frac{d\tilde{\Phi}(\zeta, \nu^2)}{d\zeta} = -\mathcal{D} \tilde{\Phi}(\zeta, \nu^2). \quad (29)$$

The function  $\Psi$  depends on  $\bar{\zeta}$  in the same way.

Generally, the function  $S_0(\nu^2, b)$  is a process-dependent and (at large- $b$ ) non-perturbative function. To get rid of it, we note that the variable  $\nu^2$  decouples from the evolution, and thus the function  $S_0$  can be absorbed into the definition of a TMD distribution without measurable effects. In fact, the physical definition of TMD distribution already includes such factors (see discussion in [7, 26]). They are build from the remnants of TMD soft factors. So, a physical TMD distribution, such as the one used to describe Drell-Yan or SIDIS processes, is defined together with an appropriate  $S_0^{\text{TMD}}$  as

$$\Phi(\zeta) = \frac{\tilde{\Phi}(\zeta, \nu^2)}{\sqrt{S_0^{\text{TMD}}(\nu^2)}}. \quad (30)$$

It is independent on  $\nu^2$  [26]. To formulate the factorization in terms of physical TMD distributions, we use the definition (30) and compensate the extra factor  $\sqrt{S_0^{\text{TMD}}}$  by an appropriate redefinition of the instant-jet TMD distribution:

$$\Psi(\bar{\zeta}) = \frac{\sqrt{S_0^{\text{TMD}}(\nu^2)} \tilde{\Psi}(\bar{\zeta}, \nu^2)}{S_0(\nu^2)}. \quad (31)$$

Note, that in a suitably defined regularization scheme (f.i.  $\delta$ -regularization [8]), the zero-bin subtraction factor  $Z.b = S^2(b)$ , and thus  $S_0^{\text{TMD}} = S_0$ . However, generally, these factors could be different in the non-perturbative regime.

## F. Final form of the factorized expression.

The final form of the factorized expression reads

$$W_{f \leftarrow h}^{[\Gamma]}(b; \ell, L; v, P, S; \mu) = \quad (32)$$

$$\left| C_H \left( \frac{\hat{p} \cdot v}{\mu} \right) \right|^2 \Phi_{f \leftarrow h}^{[\Gamma]}(b, lv^-; \mu, \zeta; P, S) \Psi(b, lv^+; \mu, \bar{\zeta}; v)$$

$$+ \mathcal{O} \left( \frac{P^-}{P^+}, \frac{1}{|b|P^+}, \frac{b}{L}, \frac{\ell}{L} \right).$$

Here, we restored all arguments of functions including the scale  $\mu$ .

There are two points in the equation (32) to be clarified. The first point is the dependence of  $\Psi$  on the variable  $\ell$ . The variable  $\ell$  appears in  $\Psi$  accompanied by the light-like vector  $\bar{n}$ , and thus can enter the function only in a scalar product with some other vector in the problem. This can only be the vector  $v$ , and thus the dependence on  $\ell$  can appear only as  $(v^+ v^- \ell \Lambda_{\text{QCD}})$  or as  $(v^+ v^- \ell / L)$  in the presence of a regularization parameter  $L$  (compare to the function  $\Phi$  where the vector  $\ell$  enters via  $(\ell v^- P^+)$ ). However, in the factorization limit both of these combinations are negligible. Thus, we conclude that the dependence on  $\ell$  is marginal,

$$\Psi(b, lv^+; \mu, \bar{\zeta}; v) = \Psi(b; \mu, \bar{\zeta}) + \mathcal{O} \left( \frac{\ell}{L}, \ell \Lambda_{\text{QCD}} \right). \quad (33)$$

This statement is also clear from the perspective of a boosted frame: boosting  $P^-/P^+ \rightarrow \infty$  one automatically gets  $v^+/v^- \rightarrow 0$ . So, the dependence on  $\ell$  is negligible, unless  $\ell$  is very large.

The second point concerns the definition of operator  $\hat{p} = -i\partial_\ell$ , acting on the function  $\Phi$ . To rewrite it in an explicit form we recall the definition of TMD distributions as functions of the momentum fraction

$$\Phi_{f \leftarrow h}^{[\Gamma]}(x, b; \mu, \zeta) = \quad (34)$$

$$\int \frac{dy^-}{2\pi} e^{-ixy^- P^+} \Phi_{f \leftarrow h}^{[\Gamma]}(b, y^-; \mu, \zeta; P, S).$$

In this representation, the positive and negative values of  $x$  are related to quark and anti-quark distributions

$$\Phi_{f \leftarrow h}^{[\Gamma]}(x, b; \mu, \zeta) = \quad (35)$$

$$\theta(x) \Phi_{f \leftarrow h}^{[\Gamma]}(x, b; \mu, \zeta) - (-1)^r \theta(-x) \Phi_{\bar{f} \leftarrow h}^{[\Gamma]}(|x|, b; \mu, \zeta),$$

where  $r$  depends on  $\Gamma$  and the Lorentz structure of the TMD. For example,  $\Gamma = \gamma^+$ ,  $r = 0(1)$  for unpolarized (spin-flip) TMDs.

Using these facts we rewrite (32) as

$$W_{f \leftarrow h}^{[\Gamma]}(b; \ell, L; v, P, S; \mu) = \quad (36)$$

$$\frac{1}{P_v} \int dx e^{ix\ell P_v} \left| C_H \left( \frac{|x|P_v}{\mu} \right) \right|^2 \Phi_{f \leftarrow h}^{[\Gamma]}(x, b; \mu, \zeta) \Psi(b; \mu, \bar{\zeta})$$

$$+ \mathcal{O} \left( \frac{P^-}{P^+}, \frac{1}{|b|P^+}, \frac{b}{L}, \frac{\ell}{L}, \ell \Lambda_{\text{QCD}} \right),$$

where  $P_v = v^- P^+$ . This is probably the most practical form of the factorization theorem, and we will use it later. The factorization statement is independent on the Dirac structure, which is standard for the TMD factorization approach. Therefore, using this expression one can describe polarized and unpolarized processes equally well.

It is important to emphasize that the size of power corrections in (36) significantly depends on  $x$ . In fact, the typical momentum scale entering factorized expressions is  $\hat{p} \sim xP$  rather than just  $P$ . Therefore, the more reliable estimation of the power corrections is  $\mathcal{O}(P^-/x^2 P^+)$ . This is a typical size of power corrections to factorization theorems for lattice observables, see e.g. the case of quasi-PDF power correction which are of order  $\mathcal{O}(\Lambda^2/x^2(pv)^2)$  as is shown in ref.[18]. Such a large power correction can undermine the applicability of the whole approach as we show later.

### III. NLO EXPRESSIONS

In this section we present the computation of elements of the factorization theorem at one loop. The calculation confirms the correctness of the construction. The calculation presented here is done in the  $\delta$ -regularization scheme [8, 27], that allows us to reuse results of earlier calculations made in [27, 28]. Our results coincide with those of [13], where they were reached in a different manner.

#### A. Hard matching coefficient

To evaluate the matching coefficient of QCD current (10) to SCET current (13) one needs to compute and compare both sides of equations (17). At the same time, one should demonstrate cancellation of collinear and soft divergences. We use  $\delta$ -regularization for collinear and soft divergences and dimensional regularization ( $d = 4 - 2\epsilon$ ) for ultraviolet divergences ( $\epsilon > 0$ ).

In the  $\delta$ -regularization scheme [8, 27] the zero-bin subtraction factor coincides with the soft factor squared

$$\text{Z.b}|_{\delta\text{-reg.}} = S^2(b). \quad (37)$$

Therefore, the matching relation at NLO turns into

$$C_H^{[1]} J_{\text{QCD}}^{[0]} = J_{\text{QCD}}^{[1]} - \Phi^{[1]} - \Phi^{[0]} \Psi^{[1]} + \Phi^{[0]} S^{[1]}, \quad (38)$$

where we omit arguments for simplicity, and use the shorthand notation for coefficients of perturbative series  $X = X^{[0]} + \alpha_s X^{[1]} + \dots$ . We have also used that  $\Psi^{[0]} = S^{[0]} = 1$ . There are four diagrams that contribute to (38), presented in fig.3. It is not the full set of diagrams contributing to each term of (38), but the contributions from the other diagrams (these are various self-energy diagrams) exactly cancel in the sum.

In  $\delta$ -regularization the diagram  $J_{\text{QCD}}$  reads

$$J_{\text{QCD}}^{[1]} = \int \frac{d^d k}{(2\pi)^d} \frac{-ig^2 C_F (\not{k} + \not{p}) \not{p} u_{\bar{n}}}{[(p+k)^2 + i\Delta][k^2 + i0][(kv) + i\Delta_v]},$$

where  $\Delta$  and  $\Delta_v$  are parameters of  $\delta$ -regularization ( $\Delta > \Delta_v > 0$ ). Evaluating this diagram in the limit  $\Delta, \Delta_v \rightarrow 0$  and  $p^+ \gg p^-$  we obtain

$$J_{\text{QCD}}^{[1]} = u_{\bar{n}} \frac{\alpha_s}{2\pi} C_F e^{-i\epsilon\pi} \left\{ \begin{aligned} & -(-(pv) - i0)^\epsilon (i\Delta)^{-\epsilon} (i\Delta_v)^{-\epsilon} \Gamma^2(\epsilon) \Gamma(1 - \epsilon) \\ & -(-v^2)^\epsilon (2i\Delta_v)^{-2\epsilon} \Gamma(2\epsilon) \Gamma(-\epsilon) + (i\Delta)^{-\epsilon} \frac{\Gamma(\epsilon)}{\epsilon(1 + \epsilon)} \\ & + (-v^2)^\epsilon (-2(pv) - i0)^{-2\epsilon} \frac{\Gamma(-1 + 2\epsilon) \Gamma(2 - \epsilon)}{\epsilon} \end{aligned} \right\} + \dots, \quad (39)$$

where the dots stand for power suppressed contributions  $\sim \Delta$ . The  $i0$ -terms are important for proper analytic continuation between the cases  $(pv) > 0$  and  $(pv) < 0$ . It reads  $(- (pv) - i0) = |pv| e^{i(\arg(pv) - \pi)}$ . The first term in brackets represents the soft divergence, whereas the second and the third terms are collinear and anti-collinear divergences. Note, that  $\epsilon > 0$  throughout and thus factors  $\Delta^{-\epsilon}$  are divergent at  $\Delta \rightarrow 0$ .

Evaluating analogously the rest of the diagrams (note, that the results for  $\Phi^{[1]}$  and  $S^{[1]}$  in  $\delta$ -regularization can be found in refs.[8, 27] and [8, 28], correspondingly) we

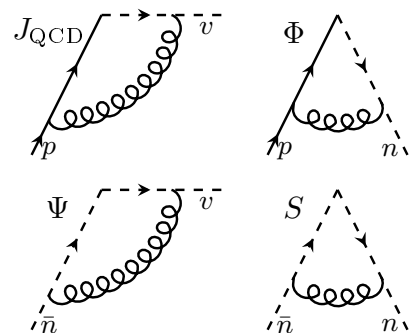


FIG. 3. Diagrams to be compute for evaluation of the hard matching coefficient. Solid (dashed) lines represent the quark field (Wilson line). In the case  $(vP) > 0$  ( $< 0$ ) the Wilson lines along  $n$  point to  $-\infty$  ( $+\infty$ ).

obtain

$$\Phi^{[1]} = u_{\bar{n}} \frac{\alpha_s}{2\pi} C_F e^{-i\epsilon\pi} \left\{ (i\Delta)^{-\epsilon} \frac{\Gamma(\epsilon)}{\epsilon(1-\epsilon)} - (\mp(pn))^\epsilon (i\Delta)^{-\epsilon} (i\delta^+)^{-\epsilon} \Gamma^2(\epsilon) \Gamma(1-\epsilon) \right\}, \quad (40)$$

$$\Psi^{[1]} = \frac{\alpha_s}{2\pi} C_F e^{-i\epsilon\pi} \left\{ -(-v^2)^\epsilon (2i\Delta_v)^{-2\epsilon} \Gamma(2\epsilon) \Gamma(-\epsilon) - (-(v\bar{n}))^\epsilon (2i\Delta_v)^{-\epsilon} (i\delta^-)^{-\epsilon} \Gamma^2(\epsilon) \Gamma(1-\epsilon) \right\}, \quad (41)$$

$$S^{[1]} = -\frac{\alpha_s}{2\pi} C_F e^{-i\epsilon\pi} (\pm 2\delta^+ \delta^-)^{-\epsilon} \Gamma^2(\epsilon) \Gamma(1-\epsilon), \quad (42)$$

where the upper sign corresponds to the geometrical configuration with  $(vP) > 0$  and the lower sign corresponds to configuration with  $(vP) < 0$ . The regularized propagators reproduce soft propagators in the soft regime, therefore, the parameters  $\Delta$  and  $\Delta_v$  are related to  $\delta^\pm$  according to

$$\delta^- = \frac{\Delta}{2p^+}, \quad \delta^+ = \frac{\Delta_v}{\pm v^-}. \quad (43)$$

The sign of  $v^-$  is the same as the sign of  $(pv)$ , and thus  $\delta^+ > 0$ . Substituting these expression into (38) we observe that each divergent sector cancels exactly (i.e. at all orders of  $\epsilon$ -expansion). Clearly, it is important to keep the proper direction of Wilson lines in mind, which leads to different signs of  $(vP)$  resulting in these cancellations. Altogether, this confirms the derived factorization theorem at NLO.

The hard-matching coefficient is

$$C_H(pv) = 1 + C_F \frac{\alpha_s}{2\pi} e^{i\epsilon(\pi - 2\arg(pv))} \times (2|pv|)^{-2\epsilon} \frac{\Gamma(-1+2\epsilon)\Gamma(2-\epsilon)}{\epsilon} + \mathcal{O}(\alpha_s^2). \quad (44)$$

Performing renormalization in the  $\overline{\text{MS}}$ -scheme we obtain

$$\left| C_H \left( \frac{vp}{\mu} \right) \right|^2 = 1 + C_F \frac{\alpha_s}{4\pi} \left( -\mathbf{L}^2 + 2\mathbf{L} - 4 + \frac{\pi^2}{6} \right) + \mathcal{O}(\alpha_s), \quad (45)$$

where  $\mathbf{L} = \ln((2|pv|)^2/\mu^2)$ . Importantly, the coefficient function is the same for  $(pv) > 0$  and  $(pv) < 0$  at this perturbative order. Nonetheless, the continuation between these regions is non-trivial, and for higher orders the coefficient functions could be different. The expression (45) coincides with the one derived for the hard coefficient function in ref.[13, 14], where the calculation has been done differently.

We have also performed the same computation with a finite-length  $H$ -Wilson line, as in (1). At  $L \rightarrow \infty$  the results coincide with (39-42) after the replacement  $\Delta_n^{n\epsilon} \rightarrow L^{-n\epsilon} \Gamma(1+n\epsilon)$ . The cancellation of divergences also takes place, although the matching relation between  $\delta^+$  and  $L$  depends on  $\epsilon$  and does not hold at higher orders of perturbation theory.

## B. Anomalous dimensions

The functions  $\Phi$  and  $\Psi$  are TMD distributions and obey the double scales evolution

$$\frac{d \ln \Phi^{[\Gamma]}(b, x^-; \mu, \zeta; P, S)}{d \ln \mu^2} = \frac{\gamma_F(\mu, \zeta)}{2}, \quad (46)$$

$$\frac{d \ln \Phi^{[\Gamma]}(b, x^-; \mu, \zeta; P, S)}{d \ln \zeta} = -\mathcal{D}(b, \mu), \quad (47)$$

and

$$\frac{d \ln \Psi^{[\Gamma]}(b, x^+; \mu, \zeta; v)}{d \ln \mu^2} = \frac{\gamma_\Psi(\mu, \zeta)}{2}, \quad (48)$$

$$\frac{d \ln \Psi^{[\Gamma]}(b, x^+; \mu, \zeta; v)}{d \ln \zeta} = -\mathcal{D}(b, \mu), \quad (49)$$

where  $\gamma_F$  and  $\gamma_\Psi$  are ultraviolet anomalous dimensions, and  $\mathcal{D}$  is the rapidity anomalous dimension. The integrability condition for these equations gives the Collins-Soper equation

$$\frac{d\gamma_F(\mu, \zeta)}{d \ln \zeta} = \frac{d\gamma_\Psi(\mu, \zeta)}{d \ln \zeta} = -\frac{d\mathcal{D}(b, \mu)}{d \ln \mu} = -\Gamma_{\text{cusp}}(\mu), \quad (50)$$

where  $\Gamma_{\text{cusp}}$  is the cusp anomalous dimension for light-like Wilson lines. The solution for ultraviolet anomalous dimensions is

$$\gamma_F(\mu, \zeta) = \Gamma_{\text{cusp}}(\mu) \ln \left( \frac{\mu^2}{\zeta} \right) - \gamma_V(\mu), \quad (51)$$

$$\gamma_\Psi(\mu, \zeta) = \Gamma_{\text{cusp}}(\mu) \ln \left( \frac{\mu^2}{\zeta} \right) - \overline{\gamma_\Psi}(\mu). \quad (52)$$

The anomalous dimension  $\gamma_V$  is known up to  $\alpha_s^3$ -order, and at LO  $\gamma_V = -6C_F\alpha_s/(4\pi)$ . The anomalous dimension  $\overline{\gamma_\Psi}$  is the finite part of the heavy-to-light anomalous dimension. Since the vertex diagram (41) contributes only to the double logarithm structure, the finite part of the anomalous dimension is twice the anomalous dimension of a heavy quark field [29]

$$\overline{\gamma_\Psi}(\mu) = 8C_F \frac{\alpha_s}{4\pi} + \mathcal{O}(\alpha_s^2). \quad (53)$$

All components of the current  $J_i$  are renormalized by a single renormalization factor,  $J_i^{\text{ren.}} = Z_J J_i$ , and thus the matrix element  $W$  is renormalized by

$$W_{\text{ren.}}^{[\Gamma]} = Z_J^2 W^{[\Gamma]}. \quad (54)$$

The corresponding anomalous dimension

$$\mu^2 \frac{dW^{[\Gamma]}}{d\mu^2} = \gamma_J W^{[\Gamma]}, \quad (55)$$

is evaluated in [30] at NNLO (for  $v^2 > 0$ ) and reads

$$\gamma_J = -3C_F \frac{\alpha_s}{4\pi} + \mathcal{O}(\alpha_s^2). \quad (56)$$

Note, that anomalous dimensions  $\gamma_J$  and  $\overline{\gamma_\Psi}$  are known in the literature related to heavy quarks physics (i.e. with

$v^2 > 0$ ) and agree with those presented here at LO. However, they could disagree at higher perturbative orders due to  $v^2 < 0$  kinematics.

The renormalization group requires

$$\frac{d \ln |C_H(pv/\mu)|^2}{d \ln \mu^2} + \frac{\gamma_V(\mu, \zeta) + \gamma_\Psi(\mu, \bar{\zeta})}{2} = \gamma_J(\mu).$$

Substituting LO anomalous dimensions and the NLO coefficient function (45), we check that this relation is satisfied if the  $\zeta$ -parameters are related by

$$\zeta \bar{\zeta} = (2\hat{p}^+ v^-)^2 \mu^2. \quad (57)$$

This fixes the relative freedom in the definition of boost-invariant variables  $\zeta$  and  $\bar{\zeta}$ . It also confirms our observation that in the absence of momentum the rapidity divergence in  $\bar{\Psi}$  are weighted by the factorization scale  $\mu$  (28).

#### IV. RATIOS OF LATTICE OBSERVABLES

The factorized expression (36) has a generic form of a TMD factorization theorem, and, therefore, it incorporates three non-perturbative functions. These are the TMD distribution  $\Phi$ , the instant-jet TMD distribution  $\Psi$ , and the rapidity anomalous dimension  $\mathcal{D}$ . The later is not explicitly presented in the formula, but enters via the scaling properties of distributions (46-49). To determine these functions one needs to measure  $W$  in a large range of parameters  $P$  and  $\ell$ . However, even in this case the function  $\Psi$ , which depends on  $\ell$  only weakly (33), would be totally correlated with  $\mathcal{D}$ .

There are two principal ways to by-pass this problem. The first approach is to obtain the values of  $\Psi$  in an independent calculation. This could be done in the perturbation theory (at small values of  $b$ ) [14], or performing a separate lattice calculation, such as the one suggested recently in ref.[31]. The second approach is to consider ratios of lattice observables, such that undesired factors (in particular the function  $\Psi$ ) cancel. This approach looks more promising because the measurements of ratios is simpler on the lattice. In addition to the cancellation of  $\Psi$  one would also profit from the cancellation of various other multiplicative factors such as lattice renormalization constants, and a corresponding reduction of systematic uncertainties for the lattice results.

In this section, we consider ratios of the form

$$R = \frac{W_{f_1 \leftarrow h_1}^{[\Gamma_1]}(b; \ell, L; v, P_1, S_1; \mu)}{W_{f_2 \leftarrow h_2}^{[\Gamma_2]}(b; \ell, L; v, P_2, S_2; \mu)}. \quad (58)$$

In such ratios the contribution of  $\Psi$  cancels, as well as a common  $\mu$ -dependence. Various properties of these ratios have been considered in [12, 13, 20, 32, 33]. In the subsequent sections, we discuss particularly interesting combinations of parameters in  $R$ , that were not yet mentioned in the literature. These combinations allow to

check the validity of the factorization theorem, and estimate the joined systematic uncertainties of the approach and the lattice computation. Additionally, we consider the case  $\ell = 0$ . The  $\ell = 0$  case is particularly simple to simulate on the lattice and has been done in refs.[32, 33]. We show that it grants access to the non-perturbative rapidity dimension.

For brevity of the formulas in this section we denote only those arguments of  $W$  that are different, assuming that all the other arguments in the ratio (58) are the same. Also, we universally denote all power corrections by

$$\mathcal{O}(\lambda) = \mathcal{O}\left(\frac{P^-}{x^2 P^+}, \frac{1}{|b| P^+}, \frac{b}{L}, \frac{\ell}{L}, \ell \Lambda_{\text{QCD}}\right). \quad (59)$$

#### A. Sign-flip

The most elementary test of the factorization theorem (36) is the measurement of the famous sign-flip of P-odd TMD distributions between the Drell-Yan and SIDIS processes [34]. SIDIS and Drell-Yan kinematics are distinguished by the sign of  $(vP)$ . Therefore, the sign-flip can be tested by turning  $v \rightarrow -v$ .

For example, considering  $\Gamma = \gamma^+$ . We have two Lorentz structures

$$W^{[\gamma^+]} = W_1 + i\epsilon_T^{\mu\nu} b_\mu s_\nu W_{1T}^\perp, \quad (60)$$

where  $\epsilon_T^{\mu\nu} = \epsilon^{+\mu\nu}$ . These structures can be independently extracted from a lattice simulation [32], and are proportional to unpolarized  $f_1$  and Sivers  $f_{1T}^\perp$  TMD distributions. The Sivers distribution is P-odd and its sign depends on the direction of the Wilson lines, in contrast to unpolarized distributions. Therefore, the following ratios should hold

$$\begin{aligned} \frac{W_1(-v)}{W_1(v)} &= 1 + \mathcal{O}(\alpha_s^2, \lambda), \\ \frac{W_{1T}^\perp(-v)}{W_{1T}^\perp(v)} &= -1 + \mathcal{O}(\alpha_s^2, \lambda). \end{aligned} \quad (61)$$

These relations are trivial at NLO due to the independence of coefficient  $|C_H|^2$  of the sign of  $(vP)$ . However, they could be violated by higher perturbative terms, if there are non-trivial effects of analytical continuation in  $(vP)$ .

Similar measurements have been performed in [32, 33], where the ratios  $W_{1T}^\perp/W_1$  (and similar for  $\Gamma = i\sigma^{+\mu}\gamma^5$ ) has been studied at different values of  $b$  and  $P$  and for different signs of  $v$ . Perfect agreement with (61) has been demonstrated.

#### B. Power suppressed terms

A great feature of lattice QCD is the possibility to measure objects unaccessible in an experiment directly.

In particular, one can compare measurements of different Lorentz structures and check the counting of the TMD factorization theorem in a completely controlled environment. The Dirac-structures of higher TMD twist must be suppressed due to dominance of the collinear components in the hadron. We have

$$\frac{W_{f\leftarrow h}^{[\Gamma_1]}}{W_{f\leftarrow h}^{[\Gamma_2]}} = \mathcal{O}(\lambda), \quad (62)$$

where  $\Gamma'_1 = 0$  and  $\Gamma'_2 = \Gamma_2$  with  $\Gamma'$  defined in (20).

Despite the apparent triviality of this statement its measurement is very important for estimation of a systematic uncertainties. In a sense, it directly measures the size of power corrections to the factorization theorem (36). This is a very valuable information, because the accessible hadron momenta in state-of-the-art lattice simulations are at most a few GeV.

### C. Non-perturbative rapidity anomalous dimension

The most exciting property of the ratios  $R$  is their exclusive sensitivity to the rapidity anomalous dimension, which was also pointed out in refs.[13, 15, 20]. The properly constructed ratio is almost independent of non-perturbative functions except the rapidity anomalous dimension. To extract  $\mathcal{D}$  one needs the ratio of  $W$ 's at different momenta

$$R_{P_1/P_2} = \frac{W_{f\leftarrow h}^{[\Gamma]}(P_1)}{W_{f\leftarrow h}^{[\Gamma]}(P_2)}. \quad (63)$$

Using (36) we get

$$R_{P_1/P_2} = \frac{P_2^+ \int dx_1 e^{ix_1 \ell v^- P_1^+} \left| C_H \left( \frac{x_1 v^- P_1^+}{\mu} \right) \right|^2 \Phi_{f\leftarrow h}^{[\Gamma']}(x_1, b; \mu, \zeta_1)}{P_1^+ \int dx_2 e^{ix_2 \ell v^- P_2^+} \left| C_H \left( \frac{x_2 v^- P_2^+}{\mu} \right) \right|^2 \Phi_{f\leftarrow h}^{[\Gamma']}(x_2, b; \mu, \zeta_2)} + \mathcal{O}(\lambda), \quad (64)$$

where  $\zeta_1 = c_0(2|x_1 v^-|P_1^+)^2$ ,  $\zeta_2 = c_0(2|x_2 v^-|P_2^+)^2$  with  $c_0$  being a constant. Note, that the scale  $\mu$  is taken to be the same in numerator and denominator in order to cancel the functions  $\Psi$ . Evolving both functions along  $\zeta$  to the same point  $\zeta_0$ , and partially canceling evolution factors we get

$$R_{P_1/P_2} = \left( \frac{P_2^+}{P_1^+} \right)^{2\mathcal{D}(b,\mu)+1} \frac{\int dx_1 e^{ix_1 \ell v^- P_1^+} \left| C_H \left( \frac{|x_1 v^-| P_1^+}{\mu} \right) \right|^2 \Phi_{f\leftarrow h}^{[\Gamma']}(x_1, b; \mu, \zeta_0) |x_1|^{-2\mathcal{D}(b,\mu)}}{\int dx_2 e^{ix_2 \ell v^- P_2^+} \left| C_H \left( \frac{|x_2 v^-| P_2^+}{\mu} \right) \right|^2 \Phi_{f\leftarrow h}^{[\Gamma']}(x_2, b; \mu, \zeta_0) |x_2|^{-2\mathcal{D}(b,\mu)}} + \mathcal{O}(\lambda). \quad (65)$$

A similar ratio is considered in details in ref.[20], where it is suggested to calculate the Fourier transform of denominator and numerator. Such a method has bright prospects, but is noticeably more demanding on the lattice side than the one discussed below. The main difficulty comes from the non-cancellation of lattice renormalization factors that, therefore, have to be computed separately. An additional, but not smaller, problem comes from the Fourier transformation in  $\ell$ , which has to be deduced from the few measurable points with  $\ell \ll L, \Lambda_{\text{QCD}}^{-1}$ . Together, these problems could result in a large systematic uncertainty.

To avoid these difficulties we suggest to consider the case  $\ell = 0$ . Roughly speaking the plain  $\ell = 0$  case corresponds to the ratio of the first Mellin moments of TMD distributions. The higher moments can be accessed by taking derivative with respect to  $\ell$ . Let us denote

$$\mathbf{R}^{(n)} = \left( \frac{P_2^+}{P_1^+} \right)^{n-2} \frac{\partial_\ell^{n-1} W_{f\leftarrow h}^{[\Gamma]}(P_1)}{\partial_\ell^{n-1} W_{f\leftarrow h}^{[\Gamma]}(P_2)} \Big|_{\ell=0}, \quad (66)$$

where the prefactor is chosen such that at  $b \rightarrow 0$  the

ratios become unity  $\mathbf{R}^{(n)} \rightarrow 1$ . These ratios give direct access to the rapidity anomalous dimension, since

$$\mathbf{R}^{(n)} = \left( \frac{P_2^+}{P_1^+} \right)^{2\mathcal{D}(b,\mu)} \mathbf{r}^{(n)} + \mathcal{O}(\lambda), \quad (67)$$

where  $\mathbf{r}^{(n)} = 1 + \mathcal{O}(\alpha_s)$ . The NLO contribution to  $\mathbf{r}^{(n)}$  is obtained using (45)

$$\mathbf{r}^{(n)} = 1 + 4C_F \frac{\alpha_s(\mu)}{4\pi} \ln \left( \frac{P_1^+}{P_2^+} \right) \left[ 1 - \ln \left( \frac{4P_1^+ P_2^+ |v^-|^2}{\mu^2} \right) - 2\mathbf{M}_{\ln|x|}^{(n),\Gamma}(b, \mu) \right] + \mathcal{O}(\alpha_s^2), \quad (68)$$

where

$$\mathbf{M}_{f(x)}^{(n),\Gamma}(b, \mu) = \frac{\int dx f(x) \cdot |x|^{-2\mathcal{D}(b,\mu)+n-1} \Phi_{f\leftarrow h}^{[\Gamma]}(x, b; \mu, \zeta_0)}{\int dx |x|^{-2\mathcal{D}(b,\mu)+n-1} \Phi_{f\leftarrow h}^{[\Gamma]}(x, b; \mu, \zeta_0)}. \quad (69)$$

It is straightforward to check that this expression is independent on  $\mu$  and  $\zeta_0$ . Therefore, it can be further simpli-

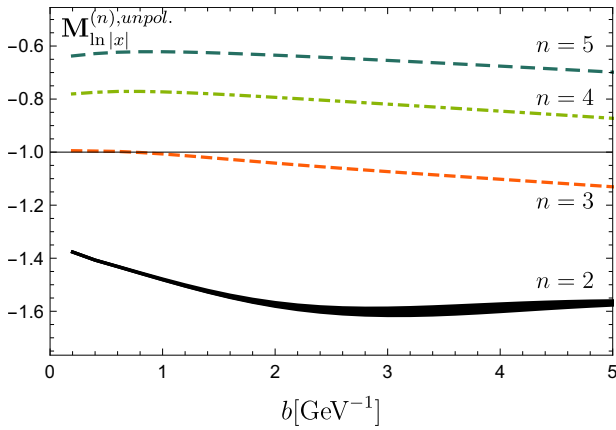


FIG. 4. Functions  $\mathbf{M}_{\ln|x|}^{(n),\Gamma}$  at different values of  $b$  and  $n$ . The computation is done for unpolarized TMD PDF (non-singlet combination  $u-d$ ) and  $\mathcal{D}$  extracted in ref.[5], at  $\mu = 3.2\text{GeV}$ . The integral over  $x$  has been cut at  $|x| > x_0$ , the thickness of the line demonstrates the resulting uncertainty, as obtained by the variation  $x_0^{-4\pm 1}$ . The case  $n = 1$  is divergent and not presented.

fied by using the optimal definition of a TMD distribution [35]. Setting  $\zeta_0 = \zeta_\mu(b)$  such that  $\Phi_{f\leftarrow h}^{[\Gamma]}(x, b; \mu, \zeta_\mu(b)) = \Phi_{f\leftarrow h}^{[\Gamma]}(x, b)$  is independent on  $\mu$ , we obtain

$$\mathbf{M}_{f(x)}^{(n),\Gamma}(b, \mu) = \frac{\int dx f(x) |x|^{-2\mathcal{D}(b,\mu)+n-1} \Phi_{f\leftarrow h}^{[\Gamma]}(x, b)}{\int dx |x|^{-2\mathcal{D}(b,\mu)+n-1} \Phi_{f\leftarrow h}^{[\Gamma]}(x, b)},$$

where  $\Phi^{[\Gamma]}(x, b)$  (without scale) is the optimal TMD distribution. The later is convenient for phenomenological extractions [3–5, 35, 36]. Let us mention, that the NNLO expression for  $\mathbf{r}^{(n)}$  can be derived using only the NLO anomalous dimensions and the finite part of  $|C_H|^2$  at NLO. Thus, it could be possibly reconstructed from already existed calculations.

The case  $n = 1$  is the most simple to measure on the lattice. However, the integrals over  $x$  in  $\mathbf{M}^{(1)}$  have unclear convergence properties. They could be divergent at  $x \rightarrow 0$  and the presence and the strength of a  $x \rightarrow 0$  divergence should depend on the Lorenz structure, flavor combination and value of  $b$ . There are two sources of such a divergence: the factor  $|x|^{-2\mathcal{D}}$  that is singular for  $\mathcal{D} > 0$ , and the TMD PDF itself.

The rapidity anomalous dimension  $\mathcal{D}$  is greater then zero for  $b \gtrsim 2e^{-\gamma_E}/\mu$ . Its asymptotic behavior is unknown, although typically it is expected to be a monotonously growing function. The value of  $\mathcal{D}$  also increases with the increase of  $\mu$ . The uncertainty of the large- $b$  behavior of modern extractions of  $\mathcal{D}$  are quite drastical [5, 6, 36]. Nonetheless, all recent extractions agree that  $\mathcal{D} > 1/2$  for  $b \gtrsim 3-4\text{GeV}^{-1}$  (here  $\mu \sim 2\text{GeV}$ ). Therefore, in this range the factor  $|x|^{-2\mathcal{D}}$  is singular.

The behavior of TMD PDFs of different kinds at small values of  $x$  has been studied in [37, 38]. It has been shown (in the large- $N_c$  approximation) that TMD PDF

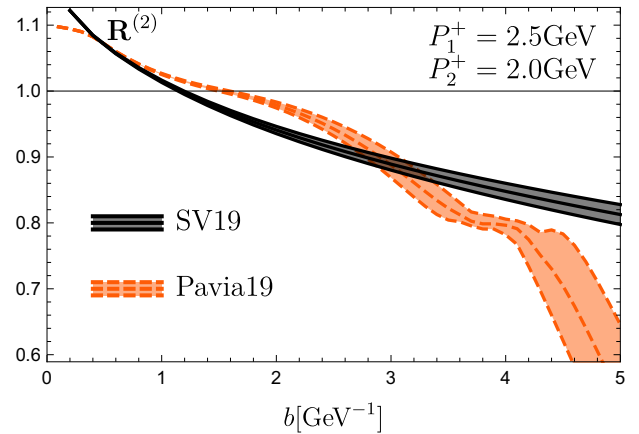


FIG. 5. Comparison of the functions  $\mathbf{R}^{(2)}$  evaluated with two different phenomenological models for rapidity anomalous dimension: “SV19” and “Pavia19” that are considered in [5] and [6], correspondingly. The uncertainty band is obtained by variation of model parameters within their uncertainty range.

behave as  $x^\alpha$ , where  $\alpha < -1$  for the unpolarized structure  $\Gamma = \gamma^+$ ,  $-1 < \alpha < 0$  for the helicity structure  $\Gamma = \gamma^+\gamma^5$ , and  $\alpha > 0$  for the transversity structure  $\Gamma = \sigma^{+\mu}$ . In each case only the leading distribution has been considered (i.e.  $f_{1L}, g_{1L}$  and  $h_1$ ). One can expect weaker singularity with a similar general hierarchy for other distributions (i.e.  $f_{1T}, g_{1T}$ , etc). Also the non-singlet combinations have weaker small- $x$  behavior (see e.g.[37]). From that we can conclude that the best convergence of the perturbative series is obtained for the flavor non-singlet transversity Dirac structure. In contrast the unpolarized case is expected to have the worst convergence properties. Using values from [5], we have tested that  $\mathbf{M}_{\ln|x|}^{(0),unpol.}$  is divergent already at  $b \gtrsim 0.5\text{GeV}^{-1}$ .

The higher- $n$  cases present a perfect environment for extraction of the non-perturbative rapidity anomalous dimension. As is shown in fig.4 the functions  $\mathbf{M}$  converge even in the unpolarized case for a wide range of values  $b$ . Moreover,  $\mathbf{M}$  is weakly dependent on  $b$ , and this dependence can be considered negligible in comparison to that of other parts of formula (68).

In fig.5 we show the function  $\mathbf{R}^{(1)}$  for typical lattice momenta  $P_1^+ = 2.5\text{GeV}$  and  $P_2^+ = 2\text{GeV}$  (and  $|v^-| = 1/\sqrt{2}$ ). The scale  $\mu$  is set to be

$$\bar{\mu} = 2|v^-| \sqrt{P_1^+ P_2^+},$$

such that the logarithm in (68) is zero. As input we take two of the most recent extractions of unpolarized TMD-PDFs and rapidity anomalous dimensions [5, 6]. The computation is done with the `artemide` package [3]. The uncertainty band is due to the uncertainty of the phenomenological parameters. The considered models have essentially different behavior at large values of  $b$ , which should be clearly distinguishable on the lattice. Let us also note that at small values of  $b$ , the limit  $R^{(n)} \rightarrow 1$  is

definitely violated. This is due to the  $(|b|P^+)^{-1}$  correction that is the part of  $\mathcal{O}(\lambda)$ .

One of the most important properties of the rapidity anomalous dimension is its universality. Therefore, the ratios  $\mathbf{R}^{(n)}$  should be almost independent of quark flavor, Dirac structure  $\Gamma$ , hadron type, and the momentum parameter  $n$  (for convergent cases). The difference between all these cases is only due to functions  $\mathbf{M}^{(n)}$ , which are smaller for higher  $n$  and suppressed at small- $x$ .

## V. CONCLUSION

In the present article, we have considered quasi-TMD operators, that can be investigated on the lattice. We pointed out the similarity of the lattice observable to the hadronic tensor of TMD processes, such as Drell-Yan or SIDIS. Using the method of soft-collinear effective field theory (SCET II) we derived the factorized expression for the lattice hadronic tensor in terms of physical TMD distributions, and the new instant-jet TMD distribution  $\Psi$  defined in (22), (31). The factorized expression generally coincides with expressions derived in [14, 15], although the route of derivation is different. We have checked the factorized expression at one-loop level and derived the hard matching coefficient at this order, which coincides with the one derived in [14]. The LO anomalous dimension could be extracted from the literature related to the heavy-quark physics, and also coincides with the results of our calculation. The present derivation is done for arbitrary Dirac structure, and can be easily extended to other interesting cases, such as gluon operators.

Since the factorization formula contains an unknown non-perturbative function  $\Psi$ , it is advantageous to consider the ratios of lattice observables with the same geometrical parameters of the operators (i.e.  $\ell$ ,  $b$ ,  $L$  and  $v$ ). In this case, many troublesome factors, such as  $\Psi$  and lattice renormalization factors, cancel. The remaining parameters, namely the Dirac structure  $\Gamma$ , hadron momen-

tum, spin and flavor, are enough to extract valuable information on TMD distributions and to estimate the uncertainties of the method. In particular, we pointed out that the ratio of the first derivatives at  $\ell = 0$  with different hadron momenta can be used to accurately determine the rapidity anomalous dimension (Collins-Soper kernel). In this case, one does not need to evaluate Fourier transformations with respect to  $\ell$ , as suggested in [13]. Considering the ratio of suppressed Dirac structures versus unsuppressed (62) allows to estimate the systematic uncertainty of the method by lattice simulations.

The hard scale of the derived factorization theorem is the hadron momentum  $P$ . Thus, one could expect that the corrections to the factorized term are  $P^{-1}$ -suppressed. However, this is only a crude estimate because the parton fields carry only a fraction of the total hadron momentum. Therefore, the true factorization scale is the parton momentum  $xP$ , which is generally much smaller. In contrast to the scattering processes, where the range of parton momentum is detected, lattice simulations involve all possible parton momenta. This leads to problems caused by low- $x$  divergences. In particular, the power corrections to lattice factorizations are  $1/x^2$ -enhanced [18]. This observation limits the application range of such factorization approaches. In particular, in the  $\ell = 0$  case (that was considered in [32, 33]), the size of corrections is very strongly dependent on the kind on operator. In certain cases (f.i. unpolarized operators) already at NLO level on can encounter divergencies.

## ACKNOWLEDGMENTS

Authors are thankful to V. Braun, X. Ji, Y. Kovchegov, Y. Liu, Y.-S. Liu, M. Schlemmer, I. Stewart, and Y.-B. Yang for stimulating discussions. This work was supported by DFG (FOR 2926 ‘‘Next Generation pQCD for Hadron Structure: Preparing for the EIC’’, project number 40824754).

- 
- [1] R. Angeles-Martinez *et al.*, Acta Phys. Polon. **B46**, 2501 (2015), arXiv:1507.05267 [hep-ph].
  - [2] A. Bacchetta, F. Delcarro, C. Pisano, M. Radici, and A. Signori, JHEP **06**, 081 (2017), arXiv:1703.10157 [hep-ph].
  - [3] I. Scimemi and A. Vladimirov, Eur. Phys. J. **C78**, 89 (2018), arXiv:1706.01473 [hep-ph].
  - [4] A. Vladimirov, JHEP **10**, 090 (2019), arXiv:1907.10356 [hep-ph].
  - [5] I. Scimemi and A. Vladimirov, (2019), arXiv:1912.06532 [hep-ph].
  - [6] A. Bacchetta, V. Bertone, C. Bissolotti, G. Bozzi, F. Delcarro, F. Piacenza, and M. Radici, (2019), arXiv:1912.07550 [hep-ph].
  - [7] J. Collins, *Foundations of perturbative QCD* (Cambridge University Press, 2013).
  - [8] M. G. Echevarria, A. Idilbi, and I. Scimemi, JHEP **07**, 002 (2012), arXiv:1111.4996 [hep-ph].
  - [9] J. C. Collins and D. E. Soper, Nucl. Phys. **B197**, 446 (1982).
  - [10] A. A. Vladimirov, Phys. Rev. Lett. **118**, 062001 (2017), arXiv:1610.05791 [hep-ph].
  - [11] B. U. Musch, P. Hagler, A. Schafer, M. Gockeler, D. B. Renner, and J. W. Negele (LHPC), *Proceedings, 25th International Symposium on Lattice field theory (Lattice 2007): Regensburg, Germany, July 30-August 4, 2007*, PoS **LATTICE2007**, 155 (2007), arXiv:0710.4423 [hep-lat].
  - [12] B. U. Musch, P. Hagler, J. W. Negele, and A. Schafer, Phys. Rev. **D83**, 094507 (2011), arXiv:1011.1213 [hep-lat].
  - [13] M. A. Ebert, I. W. Stewart, and Y. Zhao, Phys. Rev. **D99**, 034505 (2019), arXiv:1811.00026 [hep-ph].

- [14] M. A. Ebert, I. W. Stewart, and Y. Zhao, *JHEP* **09**, 037 (2019), arXiv:1901.03685 [hep-ph].
- [15] X. Ji, Y. Liu, and Y.-S. Liu, (2019), arXiv:1911.03840 [hep-ph].
- [16] X. Ji, *Phys. Rev. Lett.* **110**, 262002 (2013), arXiv:1305.1539 [hep-ph].
- [17] A. V. Radyushkin, *Phys. Rev.* **D96**, 034025 (2017), arXiv:1705.01488 [hep-ph].
- [18] V. M. Braun, A. Vladimirov, and J.-H. Zhang, *Phys. Rev.* **D99**, 014013 (2019), arXiv:1810.00048 [hep-ph].
- [19] J.-H. Zhang, J.-W. Chen, and C. Monahan, *Phys. Rev.* **D97**, 074508 (2018), arXiv:1801.03023 [hep-ph].
- [20] M. A. Ebert, I. W. Stewart, and Y. Zhao, (2019), arXiv:1910.08569 [hep-ph].
- [21] E. Eichten and B. R. Hill, *Phys. Lett.* **B234**, 511 (1990).
- [22] C. W. Bauer, D. Pirjol, and I. W. Stewart, *Phys. Rev.* **D65**, 054022 (2002), arXiv:hep-ph/0109045 [hep-ph].
- [23] C. W. Bauer, S. Fleming, D. Pirjol, and I. W. Stewart, *Phys. Rev.* **D63**, 114020 (2001), arXiv:hep-ph/0011336 [hep-ph].
- [24] C. Lee and G. F. Sterman, *Phys. Rev.* **D75**, 014022 (2007), arXiv:hep-ph/0611061 [hep-ph].
- [25] A. V. Manohar and I. W. Stewart, *Phys. Rev.* **D76**, 074002 (2007), arXiv:hep-ph/0605001 [hep-ph].
- [26] A. Vladimirov, *JHEP* **04**, 045 (2018), arXiv:1707.07606 [hep-ph].
- [27] M. G. Echevarria, I. Scimemi, and A. Vladimirov, *JHEP* **09**, 004 (2016), arXiv:1604.07869 [hep-ph].
- [28] M. G. Echevarria, I. Scimemi, and A. Vladimirov, *Phys. Rev.* **D93**, 054004 (2016), arXiv:1511.05590 [hep-ph].
- [29] D. J. Broadhurst and A. G. Grozin, *Phys. Lett.* **B267**, 105 (1991), arXiv:hep-ph/9908362 [hep-ph].
- [30] K. G. Chetyrkin and A. G. Grozin, *Nucl. Phys.* **B666**, 289 (2003), arXiv:hep-ph/0303113 [hep-ph].
- [31] X. Ji, Y. Liu, and Y.-S. Liu, (2019), arXiv:1910.11415 [hep-ph].
- [32] B. U. Musch, P. Hagler, M. Engelhardt, J. W. Negele, and A. Schafer, *Phys. Rev.* **D85**, 094510 (2012), arXiv:1111.4249 [hep-lat].
- [33] M. Engelhardt, P. Hgler, B. Musch, J. Negele, and A. Schfer, *Phys. Rev.* **D93**, 054501 (2016), arXiv:1506.07826 [hep-lat].
- [34] J. C. Collins, *Phys. Lett.* **B536**, 43 (2002), arXiv:hep-ph/0204004 [hep-ph].
- [35] I. Scimemi and A. Vladimirov, *JHEP* **08**, 003 (2018), arXiv:1803.11089 [hep-ph].
- [36] V. Bertone, I. Scimemi, and A. Vladimirov, *JHEP* **06**, 028 (2019), arXiv:1902.08474 [hep-ph].
- [37] Y. V. Kovchegov, D. Pitonyak, and M. D. Sievert, *Phys. Rev.* **D95**, 014033 (2017), arXiv:1610.06197 [hep-ph].
- [38] Y. V. Kovchegov and M. D. Sievert, *Phys. Rev.* **D99**, 054033 (2019), arXiv:1808.10354 [hep-ph].